Photochemically Driven Reverse Water-Gas Shift at Ambient Conditions mediated by a Nickel Pincer Complex

Felix Schneck,[a] Florian Schendzielorz,[a] Nareh Hatami,[a] Markus Finger,[a] Christian Würtele,[a] and Sven Schneider*[a]

Dedicated to the 150th anniversary of the Technical University Munich

Abstract: The endothermic reverse water-gas shift reaction (rWGS) for direct CO_2 hydrogenation to CO is an attractive approach to carbon utilization. However, direct CO_2 hydrogenation with molecular catalysts generally gives formic acid instead of CO as a result of the selectivity of CO_2 insertion into M–H bonds. Based on the photochemical inversion of this selectivity, several synthetic pathways are presented for CO selective CO_2 reduction with a nickel pincer platform including the first example of a photodriven rWGS cycle at ambient conditions.

The utilization of CO_2 as a C_1 building block is a major goal to establish a renewable feedstock basis. Reduction to CO is particularly attractive as a sustainable source for synthesis gas.[1] (Photo)-Electrocatalytic approaches are intensely examined with remarkable success in recent years.[1, 2] In analogy to carbon monoxide dehydrogenase (CODH), several molecular nickel electrocatalysts for CO_2 to CO and oxalate reduction have been reported.[1,2b, 3 , 4] Both for synthetic and enzymatic catalysis, metallocarboxylate species are considered key intermediates for CO selective catalysis.[5] Most recently, nickel pincer complexes were established as functional models for the [Fe_4S_4Ni]-cofactor producing CO stoichiometrically within a synthetic cycle by successive reduction ($NaC_{10}H_8$) and protonation (HBF_4) steps.[6]

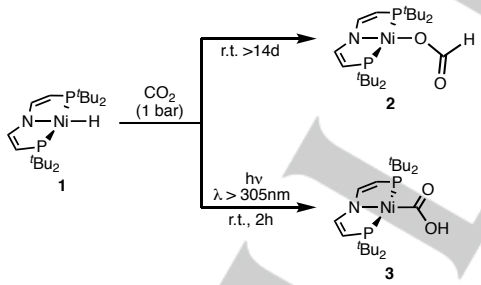

Scheme 1. *Normal* thermal vs. *abnormal* photochemical CO_2 insertion.[11]

Besides electroreduction, direct CO_2 hydrogenation is an attractive alternative, e.g. if the H_2 feed is provided from solar water splitting. Due to its endergonic nature at ambient conditions, thermally driven reverse water-gas shift (rWGS: $CO_2 + H_2 \rightarrow CO + H_2O$; Δ_rG^{298K} = +28.5 kJ mol^{-1})[7] requires high temperatures.[8] Photochemically driven rWGS at ambient conditions would be a desirable, yet currently elusive alternative. However, besides these thermochemical constraints, rWGS is also kinetically disfavored *vs.* formic acid formation with molecular CO_2 hydrogenation catalysts.[9] This selectivity is predetermined by the favored *'normal'* CO_2 insertion into catalyst M–H bonds giving formates (MO_2CH) instead of the metallacarboxylate (MCO_2H) isomers.[10] We recently reported the first well-defined *'abnormal'* CO_2 insertion reaction for the nickel(II) hydride [NiH(PNP)] (**1**; PNP = N(CHCHP*t*Bu$_2$)$_2$).[11] In contrast to the thermal insertion product [Ni(O_2CH)(PNP)] (**2**), under photochemical conditions the hydroxycarbonyl isomer [Ni(CO_2H)(PNP)] (**3**) is obtained selectively (Scheme 1). Small amounts of hydrocarbonate [Ni(OCO_2H)(PNP)] (**4**) could be attributed to slow, subsequent photochemical CO extrusion from **3** followed by CO_2 insertion. In this study, we evaluate synthetic strategies for CO selective CO_2 hydrogenation using a hydride donor, alkaline metal and ultimately directly H_2 as reductants, enabling the first example of a photodriven rWGS cycle at ambient conditions.

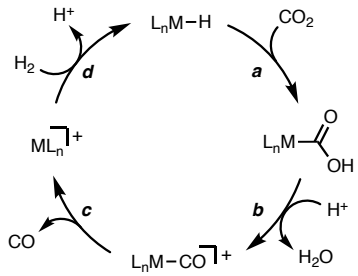

Scheme 2. Elementary steps for rWGS catalysis examined in this work.

Three additional steps are required to maintain a rWGS cycle (Scheme 2) that follows *'abnormal'* CO_2 insertion (step ***a***), i.e. water elimination (step ***b***), CO release (step ***c***), and heterolytic H_2 activation (step ***d***) to restore the parent hydride. Concerning step ***b***, protonation of **3** with strong acids like [H(OEt$_2$)$_2$][BArF] ([BArF]$^-$ = [B(C$_6$H$_3$-3,5-(CF$_3$)$_2$)$_4$]$^-$) selectively affords nickel(II) carbonyl complex [Ni(CO)(PNP)][BArF] (**5**$^{\mathbf{BArF}}$; Scheme 3). Equimolar amounts of water were quantified spectroscopically after trap-to-trap transfer of the volatiles. The square-planar complex **5**$^{\mathbf{BArF}}$ was fully characterized including single-crystal X-ray crystallography of the tetrafluoroborate salt (Figure 1). The stretching vibration of the CO ligand derived from CO_2 reduction

[a] M. Sc. F. Schneck, M. Sc. Florian Schendzielorz, B. Sc. N. Hatami, Dr. M. Finger, Dr. C. Würtele, Prof. Dr. S. Schneider
Georg-August-Universität
Institut für Anorganische Chemie
Tammannstrasse 4, 37077 Göttingen (Germany)
E-mail: sven.schneider@chemie.uni-goettingen.de

Supporting information for this article is given via a link at the end of the document.

can be assigned to a strong band in the IR spectrum at 2062 cm^{-1}.

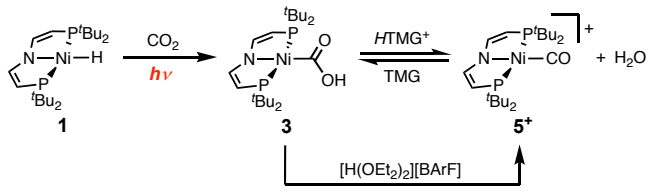

Scheme 3. Formation of CO complex **5**$^{+}$ (TMG = N,N'-tetramethylguanidine, [BArF]$^{-}$ = [B{C$_6$H$_3$-3,5-(CF$_3$)$_2$}$_4$]$^{-}$).

While this water elimination step from **3** (step ***b***) requires acidic conditions, the restoration of parent hydride **1** by H_2 heterolysis (step ***d***) should be base assisted. To maintain appropriate conditions for catalytic rWGS, a conjugate acid/base pair is needed that facilitates both steps. Several acids were therefore screened to estimate the pK_a constraint for water elimination from **3**. With tetramethylguanidinium (HTMG^{+}) in THF an equilibrium of **3** and **5**$^{+}$ was observed NMR spectroscopically (Scheme 3 and Figure 2), indicating an approximate upper bound limit (pK_α^{THF}(HTMG^{+}) = 15.3)[12] for applicable acids.

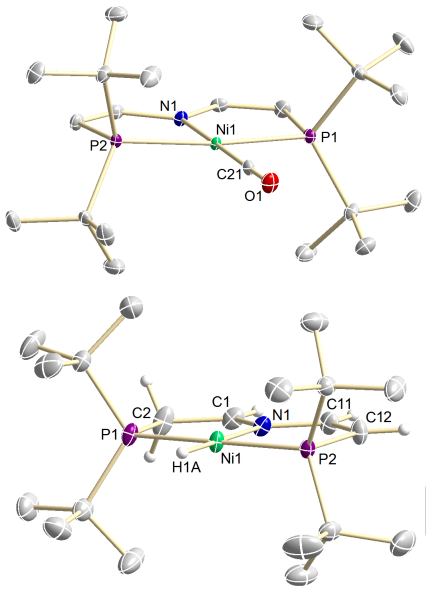

Figure 1. Molecular structure of the cations of **5**^{BF4} (top) and **6**^{O2CCF3} (below), respectively, in the crystal obtained by single crystal X-ray diffraction. Hydrogen atoms were omitted for clarity except hydride and pincer backbone hydrogen atoms of (**6**$^{+}$). Selected bond lengths (Å) and angles (°) of **5**^{BF4}: Ni1–N1 1.8694(11), Ni1–P1 2.2438(4), Ni1–P2 2.2419(4), Ni1–C21 1.7437(13); C21–Ni1–N1 179.37(6), P2–Ni1–P1 171.007(14), N1–Ni1–P1 86.02(3), N1–Ni1–P2 85.59(3). **6**^{O2CCF3}: Ni1–N1 1.9171(12), Ni1–P1 2.1556(4), Ni1–P2 2.1551(4), Ni1–H1A 1.40(2), N1–C1 1.3019(19), N1–C11 1.405(2), C1–C2 1.469(2), C11–C12 1.346(2); N1–Ni1–H1 179.0(10), P2–Ni1–P1 175.521(17), N1–Ni1–P1 87.41(4), N1–Ni1–P2 88.17(4).

Stronger acids like [HNEt$_3$]$^{+}$ (pK_α^{THF}(*H*NEt$_3^{+}$) = 12.5)[12] result in significant protonation of **1** to cationic imine hydride complex [NiH(PNP')]$^{+}$ (**6**$^{+}$, PNP' = N(CH$_2$CHP*t*Bu$_2$)(CHCHP*t*Bu$_2$)). The protonation of a carbon atom in the pincer backbone was confirmed by single-crystal X-ray diffraction (Figure 1). **6**$^{+}$ exhibits similar bond metrics as the analogous bromide complex [NiBr(PNP')]$^{+}$ that we previously reported.[13] Furthermore, the two ^{31}P NMR signals at 88.2 and 85.5 ppm ($^{2}J_{PP}$ = 215 Hz), respectively, and the ^{1}H NMR signature of the ligand backbone are in line with an enimine pincer. The acidity of **6**^{BArF} was determined by NMR titration of **1** with [HNEt$_3$][BArF] in MeCN (Figure 2). Interestingly, the pK_a value of **6**$^{+}$ (18.4) as compared with [NiBr(PNP')]$^{+}$ (pK_a^{DMSO} = 0.9) reflects a strong influence of the monodentate anionic ligand of the [NiX(PNP')]$^{+}$ platform on the ligand based acidity. Milstein and co-workers reported for a square-planar iridium(I) hydride with a related, protonated pincer ligand to directly give the respective CO complex and water upon proton transfer from the ligand backbone.[5f,14] In contrast, **6**$^{+}$ does not react with CO_2 to carbonyl complex **5**$^{+}$ both under thermal and photochemical conditions. Therefore, the pK_a of **6**$^{+}$ defines the lower limit of applicable acids for the present system. Taking these pK_a constraints into account, optimization of the conditions enabled the direct generation of **5**^{BArF} from CO_2 and imine hydride **6**^{BArF} (steps ***a*** and ***b***). Photolysis of complex **6**^{BArF} under CO_2 (1 atm) in the presence of NEt$_3$ (1 equiv.) gives **5**$^{+}$ in around 50% spectroscopic yield (Φ_{410nm} = 2.1%). Hydrocarbonate complex **4** is the only detectable side product. NMR spectroscopic monitoring of the reaction indicates initial formation of **5**^{BArF} and build-up of **4** at higher conversions. This observation suggests that the formation of hydrocarbonate **4** might be attributed to competing photochemical conversion of intermediate **3** at low acid concentrations.[11]

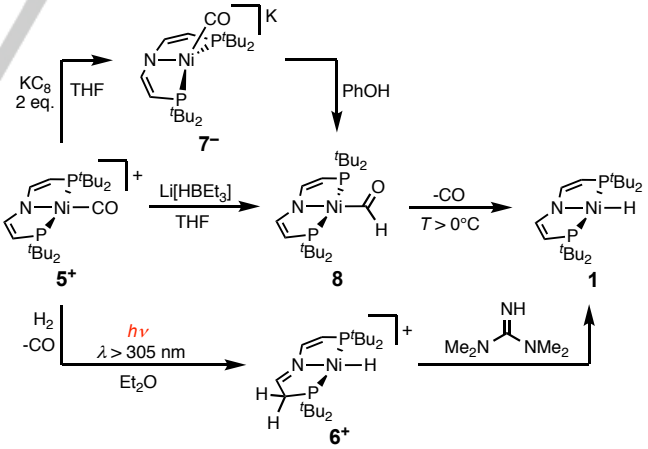

Scheme 4. Decarbonylative regeneration of hydride **1**.

Starting from carbonyl complex **5**$^{+}$, several routes are conceivable for 2e^{-}/1H^{+} reduction to restore the parent hydride **1**. Lee and coworkers most recently reported that CO elimination from a nickel(II) pincer carbonyl complex can be achieved by 2e^{-} reduction with a strong reductant (NaC$_{10}$H$_8$) and subsequent reaction with CO_2.[6d] In analogy to this work, the cyclic

voltammogram (CV) of $\mathbf{5}^{BF4}$ (Figure 2) exhibits two reversible reduction waves at E_1^0 = -1.31 V (*vs.* Fc/Fc$^+$) and E_2^0 = -2.22 V, respectively. Importantly, in the presence of phenol the more cathodic wave turns irreversible and shifts increasingly anodically with rising acid concentrations. This observation is suggestive of an *EC*-mechanism for the second reduction, such as proton coupled electron transfer (PCET). This interpretation is confirmed by chemical reduction. Nickel(I) complex [Ni^I(CO)(PNP)] (ν_{CO} = 1910 cm^{-1}), which we previously reported from reaction of [Ni(PNP)] with CO,[11] is obtained upon reduction of $\mathbf{5}^+$ with Mg. Reduction of [Ni^I(CO)(PNP)] with 1 eq. $NaC_{10}H_8$ selectively gives a diamagnetic species, which exhibits C_s symmetry below –30°C on the ^{1}H NMR timescale. The ^{13}C{^{1}H} NMR signal at 208 ppm ($^2J_{C\text{-}P}$ = 18.8 Hz) and the strong IR band at 1776 cm^{-1} further support the assignment as strongly reduced [Ni(CO)(PNP)]$^-$ ($\mathbf{7}^-$; Scheme 4). Reduction with KC_8 afforded the crystallographic characterization of [$\mathbf{7}^K$(OEt$_2$)]$_2$ (Figure 3). The potassium cations of the dimeric structure are coordinated by the pincer enamido π system, the CO ligand of both fragments and an additional diethylether ligand. The {Ni(CO)(PNP)}$^-$ core exhibits strongly distorted tetrahedral nickel coordination (τ_4 = 0.64),[15] resembling the anionic carbonyl pincer complex reported by Lee and co-workers (τ_4 = 0.70).[6d, 16] In contrast, our nickel(I) complex [Ni(CO)(PNP)] features much weaker distortion (τ_4 = 0.24) from square-planar geometry as compared with related nickel(I) PNP carbonyl complexes (τ_4 = 0.37–0.50).[6d,11, 17] Addition of 2 eq [HNEt$_3$][BArF] to *in situ* generated $\mathbf{7}^-$ (from $\mathbf{5}^+$ and KC_8) results in immediate consumption of the carbonyl complex and formation of parent hydride **1** as main product in around 50% spectroscopic yield besides other unidentified species (Supporting Information, Figure S22).

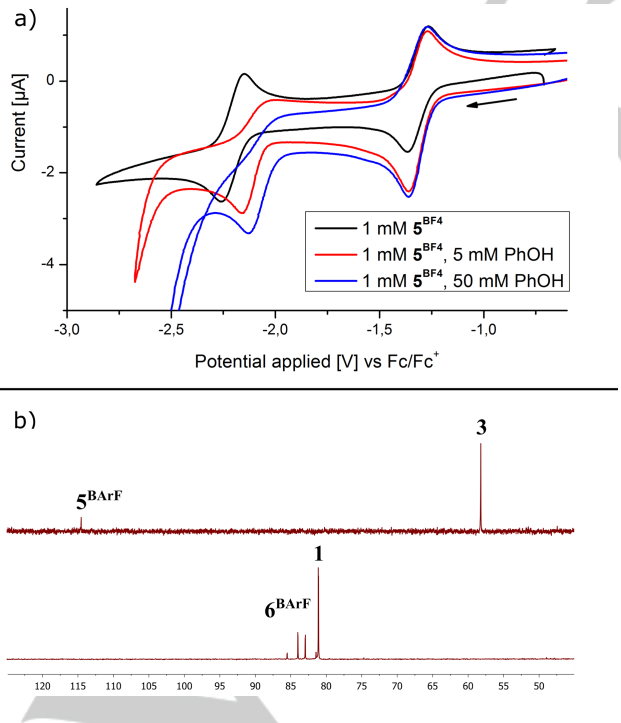

Figure 2. (a) Cyclic voltammogram of complex $\mathbf{5}^{BF4}$ (c = 1 mM) in THF in the presence of 0 eq (black), 5 eq (red) and 50 eq (blue) phenol, respectively (conditions: 0.1 M [*n*-Bu$_4$N][PF$_6$], glassy carbon working electrode, Pt counter electrode, Ag wire reference electrode). (b) top: ^{31}P{^{1}H} NMR spectrum of **3** in the presence of 1 eq [HTMG][BArF] in THF. Bottom: ^{31}P{^{1}H} NMR spectrum of **1** in the presence of 1 eq [HNEt$_3$][BArF] in MeCN ([BArF]$^-$ = [B(C$_6$H$_3$-3,5-(CF$_3$)$_2$)$_4$]$^-$).

This regeneration of parent **1** by stepwise 2e$^-$/1H$^+$ reduction of $\mathbf{5}^+$ is associated with an intermediate that exhibits a distinct triplet resonance at 14.08 ppm ($^3J_{H\text{-}P}$ = 12.9 Hz, Figure S21) in the ^{1}H NMR spectrum. The intermediate could be identified by concerted 2e$^-$/1H$^+$-PCET to $\mathbf{5}^+$ using Li[HBEt$_3$] as hydride source (Scheme 4). Monitoring the selective formation of hydride complex **1** by means of NMR spectroscopy confirms the formation of the same intermediate (^{31}P NMR: δ = 60.0 ppm), which is stable in THF up to about 0 °C and converts to **1** at r.t. (Figure S16). The strongly downfield shifted resonance in the ^{1}H (δ = 14.10 ppm, $^3J_{HP}$ = 12.2 Hz) and ^{13}C{^{1}H} NMR (δ = 262.9 ppm, $^2J_{CP}$ = 21.7 Hz) spectra evidence the formation of formyl complex [Ni(COH)(PNP)] (**8**; Scheme 4) prior to decarbonylation to parent complex **1**. Notably, formyl complexes play a key role in CO reduction but have only been observed for the higher homologues of nickel.[18]

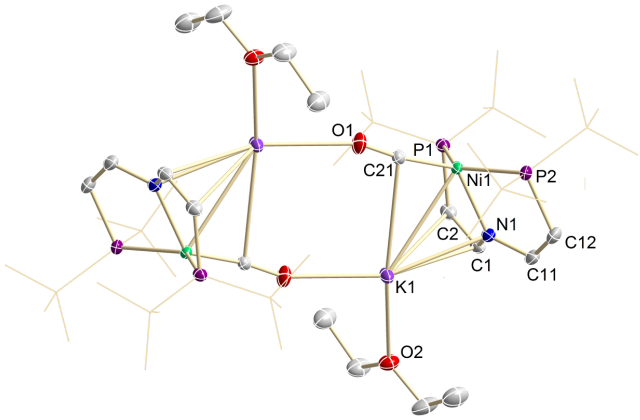

Figure 3. Molecular structure of the of $\mathbf{7}^K$·**OEt$_2$** in the crystal obtained by single crystal X-ray diffraction. Hydrogen atoms were omitted for clarity. Selected bond lengths (Å) and angles (°): Ni1–N1 2.0202(10), Ni1–P1 2.2645(4), Ni1–P2 2.2748(4), Ni1–C21 1.7076(12); O1–C21 1.1863(15); C1–C2 1.3581(19); C11–C12 1.351(2); C21–Ni1–N1 131.0(5), P2–Ni1–P1 138.734(13), N1–Ni1–P1 83.77(3), N1–Ni1–P2 84.93(3); O1–C21–Ni1 172.09(11).

These two routes for the regeneration of parent **1** close a full cycle for CO_2 to CO reduction. However, either complex hydride donors are required, reducing the atom economy of the reaction, or strong reductants, as in Lee's related example. As a more sustainable alternative, photodriven rWGS with direct utilization of H_2 as reducing agent was therefore examined. Neither hydrocarbonate **4** nor the carbonyl complex $\mathbf{5}^+$ react with H_2 at room temperature up to pressures of $p(H_2)$ = 10 bar without irradiation. However, photolysis of $\mathbf{5}^+$ under an atmosphere of H_2 (1 atm, λ > 305 nm, r.t.) results in highly selective formation of $\mathbf{6}^+$ with a quantum yield of Φ_{337nm} = 0.5% (Scheme 4) upon metal-ligand cooperative H_2 heterolysis with proton transfer to the pincer backbone. The release of CO was confirmed by gas

chromatography (Supporting Information, Figure S25). Notably, metal-ligand cooperativity (MLC) has proven to be conceptually highly useful for nickel catalyzed electrochemical proton reduction/hydrogen oxidation.[19] Photochemical H_2 activation with $\mathbf{5^+}$ requires the use of weakly coordinating solvents (diethyl ether, fluorobenzene) presumably to avoid inhibition by solvent binding to a {Ni(PNP)}-fragment after CO release. Intermediates, such as a dihydrogen complex, were not observed.

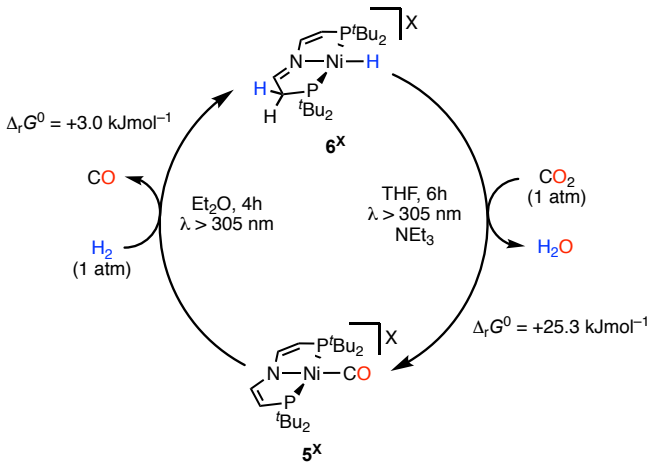

Scheme 5. Two-step photodriven rWGS cycle (X^- = $B(C_6H_3\text{-}3,5\text{-}(CF_3)_2)_4^-$). Reaction free energies refer to computed values (DLNPO-CCSD(T)//D3BJ-RIJ-PBE/def2-SVP(SMD(Et_2O)).

This reactivity enabled the establishment of a simple, 2-step cycle (Scheme 5). Hydrogenolytic decarbonylation of $\mathbf{5^+}$ is followed by NEt_3 assisted CO_2 reduction and water elimination. Both steps require photochemical conditions (λ > 305 nm). When carried out in a closed vessel, the reaction rate of CO release drops at high conversion, suggesting reversible binding of H_2 vs. CO. In fact, this decarbonylation branch of the cycle ($\mathbf{5^+}$ + H_2 → $\mathbf{6^+}$ + CO) was computed to be almost thermoneutral (ΔG_0^{298K} = +3.0 kJmol^{-1}; DLNPO-CCSD(T)//D3BJ-RIJ-PBE/def2-SVP(SMD(Et_2O)). In turn, the computations indicate strongly endergonic (ΔG_0^{298K} = +25.3 kJmol^{-1}), hence photochemically driven CO_2 reduction and water elimination ($\mathbf{6^+}$ + CO_2 → $\mathbf{5^+}$ + H_2O).

In summary, several strategies were evaluated for photochemical CO_2 to CO conversion mediated by a nickel PNP pincer platform. Besides the sequential $2e^-/1H^+$ reduction/protonation or concerted utilization of a molecular hydride source, which are well established routes in CO_2 reduction, we demonstrated a simple, 2-step, photodriven rWGS cycle at room temperature as a proof-of-principle. CO_2 reduction is mediated by a nickel complex and relies on the inversion of the CO_2 insertion selectivity under photochemical conditions. Furthermore, the functional pincer ligand proved instrumental for H_2 heterolysis by MLC. Evaluation of the pK_a constraints for the proton transfer steps showed that bases like NEt_3 provide suitable conjugate acid/base pairs as a prerequisite for catalysis. Future work will be dedicated to establish catalytic rWGS at ambient conditions.

Acknowledgements

This work was supported by grants from the European Research Council (ERC Grant Agreement 646747) and the Deutsche Forschungsgemeinschaft (CRC 1073, Project C07).

Keywords: Hydrogenation • CO_2 • Nickel • Pincer Ligand • Photochemistry

[1] A. M. Appel, J. E. Bercaw, A. B. Bocarsly, H. Dobbek, D. L. DuBois, M. Dupuis, J. G. Ferry, E. Fujita, R. Hille, P. J. A. Kenis, C. A. Kerfeld, R. H. Morris, C. H. F. Peden, A. R. Portis, S. W. Ragsdale, T. B. Rauchfuss, J. N. H. Reek, L. C. Seefeldt, R. K. Thauer, G. L. Waldrop, *Chem. Rev.* **2013**, *113*, 6621–6658.

[2] (a) M. Rakowski DuBois, D. L. DuBois, *Acc. Chem. Res.* **2009**, *42*, 1974–1982. (b) J. Schneider, H. Jia, J. T. Muckerman, E. Fujita, *Chem. Soc. Rev.* **2012**, *41*, 2036–2051. (c) C. M. Constentin, M. Robert, J.-M. Savéant, *Acc. Chem. Res.* **2015**, *48*, 2996–3006. (d) S. Berardi, S. Drouet, L. Francàs, C. Gimbert-Suriñach, M. Guttentag, C. Richmond, T. Stoll, A. Llobet, *Chem. Soc. Rev.* **2014**, *43*, 7501–7519.

[3] M. Rudolph, S. Dautz, E.-G. Jäger, *J. Am. Chem. Soc.* **2000**, *122*, 10821-10830.

[4] (a) B. Horn, C. Limberg, C. Herwig, B. Braun, *Chem. Commun.* **2013**, *49*, 10923-10925. (b) P. Zimmermann, C. Limberg, *J. Am. Chem. Soc.* **2017**, *139*, 4233–4242.

[5] (a) M. Hammouche, D. Lexa, M. Momenteau, J.-M. Saveant, *J. Am. Chem. Soc.* **1991**, *113*, 8455–8466. (b) E. Fujita, L. R. Furenlid, M. W. Renner, *J. Am. Chem. Soc.* **1997**, *119*, 4549–4550. (c) S. Sato, T. Morikawa, T. Kajino, O. Ishitani, *Angew. Chem. Int. Ed.* **2013**, *52*, 988–992. (d) M. Bourrez, M. Orio, F. Molton, H. Vezin, C. Duboc, A. Deronzier, S. Chardon-Noblat, *Angew. Chem. Int. Ed.* **2014**, *126*, 240–243. (e) K. Garg, Y. Matsubara, M. Z. Ertem, A. Lewandowska-Andralojc, S. Sato, D. J. Szalda, J. T. Muckerman, E. Fujita, *Angew. Chem. Int. Ed.* **2015**, *54*, 14128–14132. (f) M. Feller, U. Gellrich, A. Anaby, Y. Diskin-Posner, D. Milstein, *J. Am. Chem. Soc.* **2016**, *138*, 6445–6454. (g) P. Zimmermann, S. Hoof, B. Braun-Cula, C. Herwig, C. Limberg, *Angew. Chem. Int. Ed.* 10.1002/anie.201802655.

[6] (a) C. Yoo, J. Kim, Y. Lee, *Organometallics* **2013**, *32*, 7195–7203. (b) C. Yoo, Y. Lee, *Chem. Sci.* **2017**, *8*, 600–605. (c) C. Yoo, Y. Lee, *Angew. Chem. Int. Ed.* **2017**, *56*, 9502–9506. (d) D. Sahoo, C. Yoo, Y. Lee, *J. Am. Chem. Soc.* **2018**, *140*, 2179–2185.

[7] A. D. King, R. B. King, D. B. Yang *J. Am. Chem. Soc.* **1980**, *102*, 1028–1032.

[8] Y. A. Daza, J. N. Kuhn, *RSC Adv.* **2016**, *6*, 49675.

[9] (a) S. Chakraborty, P. Bhattacharya, H. Dai, H. Guan, *Acc. Chem. Res.* **2015**, *48*, 1995–2003. (b) R. C. Cammarota, M. V. Vollmer, J. Xie, J. Ye, L. C. Linehan, S. A. Burgess, A. M. Appel, L. Gagliardi, C. C. Lu, *J. Am. Chem. Soc.* **2017**, *139*, 14244–14250.

[10] (a) P. G. Jessop, T. Ikariya, R. Noyori, *Chem. Rev.* **1995**, *95*, 259–272. (1995). (b) P. G. Jessop, F. Joó, C.-C. Tai, *Coord. Chem. Rev.* **2004**, *248*, 2425–2442. (c) W.-H. Wang, Y. Himeda, J. T. Muckerman, G. F. Manbeck, E. Fujita, *Chem. Rev.* **2015**, *115*, 12936–12973. (d) E. Alberico, M. Nielsen, *Chem. Commun.* **2015**, *51*, 6714–6725.

[11] F. Schneck, J. Ahrens, M. Finger, A. C. Stückl, C. Würtele, D. Schwarzer, S. Schneider, *Nat. Commun.* **2018**, 9, 1161.

[12] T. Rodima, I. Kaljurand, A. Pihl, V. Mäemets, I. Leiro, I. A. Koppel, *J. Org. Chem.* **2002**, *67* 1873–1881.

[13] F. Schneck, M. Finger, M. Tromp, S. Schneider, *Chem. Eur. J.* **2017**, *23*, 33–37.

[14] A. Anaby, M. Feller, Y. Ben-David, G. Leitus, Y. Diskin-Posner, L. J. W. Shimon, D. Milstein, *J. Am. Chem. Soc.* **2016**, *138*, 9941–9950.

[15] L. Yang, D. R. Powell, R. P. Houser, *Dalton Trans.* **2007**, 955−964.

[16] This τ_4 value for Lee's complex refers to a dimeric, Na-bridged structure similar to that of **7^{K}**. The structure of the respective free anion $\{Na^0(CO)L]^-$ was reported with τ_4 = 0.64 (ref. 6d).

[17] C. Yoo, S. Oh, J. Kim, Y. Lee, *Chem. Sci.* **2014**, *5*, 3853–3858.

[18] (a) L. Schwartsburd, E. Poverenov, L. J. W. Shimon, D. Milstein, *Organometallics* **2007**, *26*, 2931–2936. (b) D. Vuzman, E. Poverenov, Y. Diskin-Posner, G. Leitus, L. J. W. Shimon, D. Milstein, *Dalton. Trans.* **2007**, 5692–5700.

[19] (a) A. D. Wilson, R. H. Newell, M. J. McNevin, J. T. Muckerman, M. R. DuBois, D. L. DuBois, *J. Am. Chem. Soc.* **2006**, *128*, 358–366. (b) T. He, N. P. Tsvetkov, J. G. Andino, X. Gao, B. C. Fullmer, K. G. Caulton, *J. Am. Chem. Soc.* **2010**, *132*, 910–911. (c) R. M. Bullock, M. L. Helm, *Acc. Chem. Res.* **2015**, *48*, 2017–2026.

Entry for the Table of Contents

COMMUNICATION

Let there be light: A simple, two-step photodriven reverse-water-gas-shift (rWGS) cycle at ambient temperature and pressure is reported. The CO_2 to CO hydrogenation is mediated by a molecular nickel hydride. The reaction relies on photochemical abnormal CO_2 insertion into the Ni–H bond and cooperative, heterolytic H_2-activation by the metal and the functional pincer ligand.

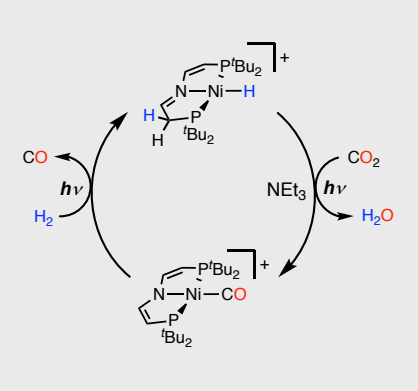

*F. Schneck, F. Schendzielorz, N. Hatami, M. Finger, C. Würtele, S. Schneider**

Page No. – Page No.

Photochemically Driven Reverse Water-Gas-Shift at Ambient Conditions